

Magnet Design Report

Dipole magnet D1

Author	Checked by – date	Approved by – date
Davide Castronovo		

Table of Contents

1	INTRODUCTION.....	3
1.1	ACRONYMS AND ABBREVIATIONS.....	3
2	REQUIREMENTS AND DESIGN GUIDELINES.....	3
3	MAGNETS DESIGN.....	4
3.1	INTRODUCTION	4
3.2	POWER CONVERTER MAXIMUM CURRENT	5
3.3	MAGNET PARAMETERS.....	5
3.4	MAGNET YOKE LAYOUTS.....	5
3.5	COIL DESIGN.....	6
4	MAGNETIC FIELD CALCULATION	8
4.1	YOKE DESIGN	8
4.2	2D5 SIMULATIONS.....	8
4.3	FIELD HOMOGENEITY OPTIMIZATION	9
4.4	2D5 FIELD HOMOGENEITY OPTIMIZATION.....	9
4.5	3D SIMULATIONS.....	11
4.6	3D FIELD HOMOGENEITY OPTIMIZATION.....	12
5	D1 SUMMARY	14
5.1	CONCEPTUAL 3D MODEL	14
5.2	Q5 MAGNETIC PERFORMANCES.....	15
6	ANNEX.....	16
6.1	MATERIAL USED FOR MAGNETIC SIMULATIONS	16
6.2	DIPOLE MODEL.....	16

1 INTRODUCTION

The dogleg part of the Accelerator-to-Target (A2T) section of the ESS accelerator contains two vertical dipole magnets, which bring the beam from the accelerator tunnel level up to the level of the target where the beam is focused and transported to the target in a straight section using six quadrupole magnets of type Q8. This document describes the conceptual design of the dipoles, which are referred to as type D1.

The dipoles are normal-conducting and will operate in DC mode. In addition to bending the beam, the dipole magnet is designed to accommodate a special vacuum chamber with a straight-out beam port, allowing the beam transport towards the tuning beam dump, when the dipole is powered-off. Due to an expected remnant field when the dipole is powered-off, a correction coil may be added to nullify that field and to allow the beam to pass straight to the tuning beam dump.

1.1 ACRONYMS AND ABBREVIATIONS

Acronym	Explanation
DC	Direct Current
PC	Power Converter
GFR	Good Field Region
FFT	Fast Fourier Transform
GUI	Graphical User Interface
CAD	Computer Aided Design
ABS	Absolute Value
Pw	Power

2 REQUIREMENTS AND DESIGN GUIDELINES

Since these magnets have a large vacuum chamber, i.e. the aperture gap is large, special attention has been paid to the ampere-turns calculations. Another attention has been paid to limit, in a reasonable way, the overall dimensions of the yoke.

In order to make feasible also the realization of the coils cooled by water, the maximum current value has been set both to reduce the number of turns as well as to minimize the coil overall dimensions.

More in detail, to minimize as much as possible the power consumptions, D1 must adopt conductors that have a cross section area such as to keep the maximum current density lower than 4.5 A/mm^2 . At the same time, the conductors must have a cooling channel with a diameter sufficiently large in order to reduce the required liquid velocity and thus limiting the pressure drop in the cooling circuit.

To obtain the required total pressure drop (< 5 Bar), the number of branches have been set and the liquid inlet and outlet interfaces must be defined.

To minimize the eddy current in the iron during the magnet cycling reset or the setting of the current value, the yoke will be made of laminated steel sheets with a thickness of 1.0 mm.

Table 1 reports the requirements for D1 as reported in DOORS.

Table 1: **D1** DOORS requirements

ID	Parameter		value	unit
4679	Overall length	\leq	2200	mm
4681	Gap between the poles	\geq	116	mm
4683	Magnetic length along the central trajectory	$=$	1800	mm
4686	Bending angle for the central trajectory	$=$	4	deg
4687	Bending radius for the central trajectory	$=$	25783	mm
4689	Nominal magnetic field B_0	$=$	0.36	T
4690	Operating Range of the magnetic field B	$=$	$0.14 \div 0.4$	T
4691	Maximum magnetic field B_{MAX}	\geq	0.43	T
4692	Good field region radius	\geq	35	mm
4693	Magnetic field integral uniformity	\leq	± 0.1	%
4702	Remnant magnetic field	\leq	5	Gauss

Since the commercial low carbon steel has a residual field typically between $8 \div 20$ Gauss, the required remnant magnetic field (≤ 5 Gauss) must be obtained by an opposite excitation or by a degaussing cycling. The first one can be obtained by the polarity switch of the main PC; the second one can be realized by switching on a secondary 4 quadrant PC by what is possible to excite the magnet by a decreasing wave form.

3 MAGNETS DESIGN

3.1 INTRODUCTION

The magnetic designs started with a pre-design where all the parameters were calculated by theoretical formulas and excel work-sheets. In order to estimate further real 3D parameters such as magnetic length, yoke saturation and magnet inductance, 3D electromagnetic simulations had been run.

After the pre-design, the final magnetic design optimized the multipole components and the field distribution in order to reach all the specifications within the required ranges.

3.2 POWER CONVERTER MAXIMUM CURRENT

In order to reduce as much as possible the types of power converters, D1 will be designed with the same Q8 maximum current value, which is 400 A.

Since in this case the degaussing current value could be between 0.3÷1.2 A, and that these values are too small for a 400 A PC, the reduction of the remnant field by switching on a secondary 4 quadrant PC is preferable.

To make feasible the use of a cooling circuit with no more than 4 branches (two for each coil), the pre-design have used a square conductor section (Cond.WH) with a sufficiently big cooling channel diameter (Cond.Ø).

3.3 MAGNET PARAMETERS

Table 2 lists magnet parameters and performances calculated by VF Opera 3D.

Table 2: Magnet parameters and performances

Parameters			unit
Gap	=	116	mm
Yoke overall width	=	606	mm
Yoke overall height	=	742	mm
Good field region radius r_0	=	35	mm
Yoke length	=	1792	mm
Coils overall length	≤	1990	mm
Magnetic length L_{eff} at nominal I_c	=	1802	mm
Maximum integrated field on	=	0.836	Tm
Content B_n / B_1 (with $n = 2$ and 3) at r_0	<	0.08	%
Inductance	=	862	mH

3.4 MAGNET YOKE LAYOUTS

In order to reduce the eddy current effect (during the possible startup, the reset cycling or the setting of the current value) it's preferable that the yokes are made of laminated steel sheets of 1.0 mm thickness that are glued together. The recommended steel type will be cold-rolled, final annealed, no grain-oriented electrical steel. The $B(H)$ curve of such a material shall be better or equal to the $B(H)$ curve used for the magnetic field calculations (VF Opera "tenten", see Table 8). The steel strips are pre-coated on both sides with a thin layer (5 to 8 μm) of epoxy resin. This layer provides the required surface insulation between the laminations and serves at the same time as a bonding agent between them.

After stacking and curing, the packing factor¹ of each quadrant shall be greater than or equal to 97% (low margin respect the typically value of 98%).

Table 3 lists all yoke parameters. Note that the yoke weight was calculated by the typically value of the packing factor, which is 0.98.

Table 3: Yoke parameters

Parameters		unit
Type	Straight H-type	
Yoke	Laminated	
Simulated material	VF Opera - tenten	
Simulated packing factor	97	%
Yoke overall width	606	mm
Yoke overall height	742	mm
Yoke length	1792	mm
Yoke volume	588	dm ³
Yoke mass (calculated by $0.98 \cdot \rho_{Fe}$)	~ 4500	kg

3.5 COIL DESIGN

The coils conductor shall be made of high conductivity (OFHC-type) copper. The wire shall be wrapped by two consecutive layers of insulating tapes; the first one of Kapton® polyamide, and the second one of fiberglass, for a total insulation thickness of about 0.5 mm. The coils shall be vacuum-impregnated using a radiation-resistant thermosetting epoxy resin. The final insulation must be able to withstand a suitable test voltage.

The coil parameter calculations assumed a resistivity of $1.72 \times 10^{-8} \Omega m$ at 20°C. Due to the relatively high current density, the coils have to be water-cooled. In order to reduce the total pressure drop (< 5 bar), the cooling circuit will have four branches, two for each coil. Each coil shall be equipped with thermal switches for protection against overheating. Two thermal switches must be positioned on the outlet connection of each branch, for a total of four thermal switches for each coil.

With a maximum current value of 400 A, the coils are made of a copper conductor with a cross section of 12 x 12 mm and with a cooling channel diameter of 7 mm; the resulting conducting area is of ~ 105 mm². The proposed coils geometry will be the simple race track type with 54 turns for each one (54 x 2 = 108 total turns), of which 9 turns on height and 6 turns on width. Figure 1 shows the proposed coil conductor winding, terminals and branches subdivision.

¹ The packing factor is defined as the ratio of the mass of the steel of the laminated yoke quadrant and the mass of a solid yoke quadrant of the same volume and of the same material density.

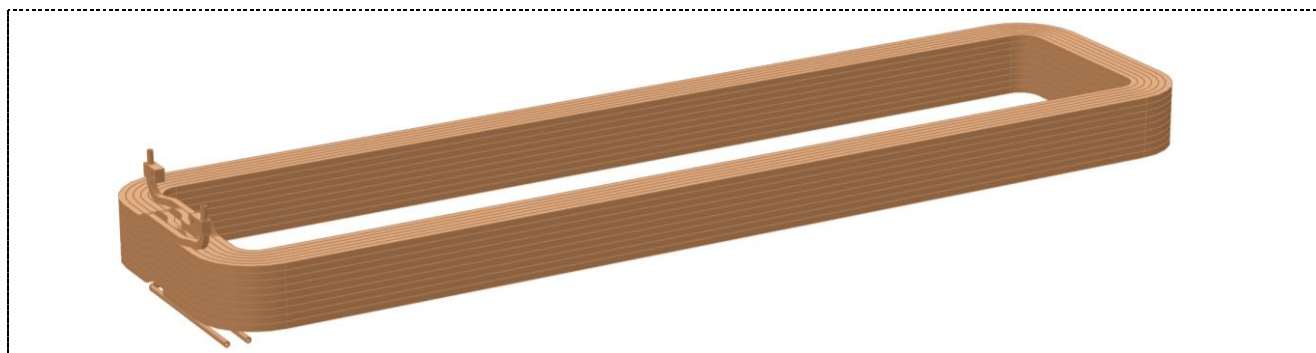


Figure 1: Coil conductor winding, terminals and branches subdivision.

Table 4 lists all coil parameters and provides an overview of all relevant power converter and cooling system parameters. Note that the minimum required coolant flow is calculated at the maximum required current I_{RMax} so that a temperature rise of 25°C is obtained.

Table 4: Coil parameters; in parenthesis the values at the minimum required coolant flow

Parameters		unit
Type	Racetrack	
Cooling	demineralized water	
Conductor cross section	12 x 12 mm - hole Ø 7 mm = 105	mm ²
Number of turns for one coil	54	#
Number of turns on width	6	#
Number of turns on height for one coil	9	#
Space between coil and yoke	12	mm
Maximum current density j	3.82	A/mm ²
Conductor length for one coil	247	m
Resistance for one coil at 22°C	40.6	mΩ
Coil overall length	1990	mm
Mass for one coil	~ 230	Kg
PC maximum required current I_{RMax}	371	A
Coolant total flow (<i>minimum required</i>)	12.0 (7.5)	l/min
Cooling power dissipation at I_{RMax}	11.7 (12.0)	kW
Cooling branches number	4 (2 for each coil)	#
Coolant temperature rise at I_{RMax}	14 (25.0)	°C
Coolant velocity on each branch	1.30 (0.75)	m/s
Coolant pressure drop	4.5 (1.7)	bar

4 MAGNETIC FIELD CALCULATION

4.1 YOKE DESIGN

Since the required angle is 4° and the arc length is 1800 mm, the yoke of D1 could be design curved or straight. The evaluation of these two types has taken into account their effect in terms of overall dimensions and feasibility (required mechanical precisions and simplicity of realization).

As regards the straight type, in order to obtain the field quality specification, the magnet must have no pole shimming and a larger GFR such as to cover the offset due to the distance between the cord and the arc of the nominal trajectory, which in this case is 15.7064 mm. Since the good field range on X is ± 35 mm while the minimum gap required is 116 mm, it should be noted that the field quality specification leads a pole width which covers the above defined offset comfortably.

As for the curved type, however, the possibility of reducing the pole width by a shimming of the pole profile is inadequate for the same reason as the size of the gap relative to the good field range on X. In this case, it should be noted that the realization of the curved yoke and the curved coil windings requires costs and possible issues for this unjustified.

Since for both the types the goal was to decrease, as much as possible, the transversal dimension (and consequently the quantity of iron) and the two types differ only on the pole width, the straight type has been resulted preferable.

4.2 2D5 SIMULATIONS

In order to run the optimization of the parameters with faster simulations, Opera 3D has been employed in a pseudo bi-dimensional way, a kind of 2.5D, that we have named 2D5.

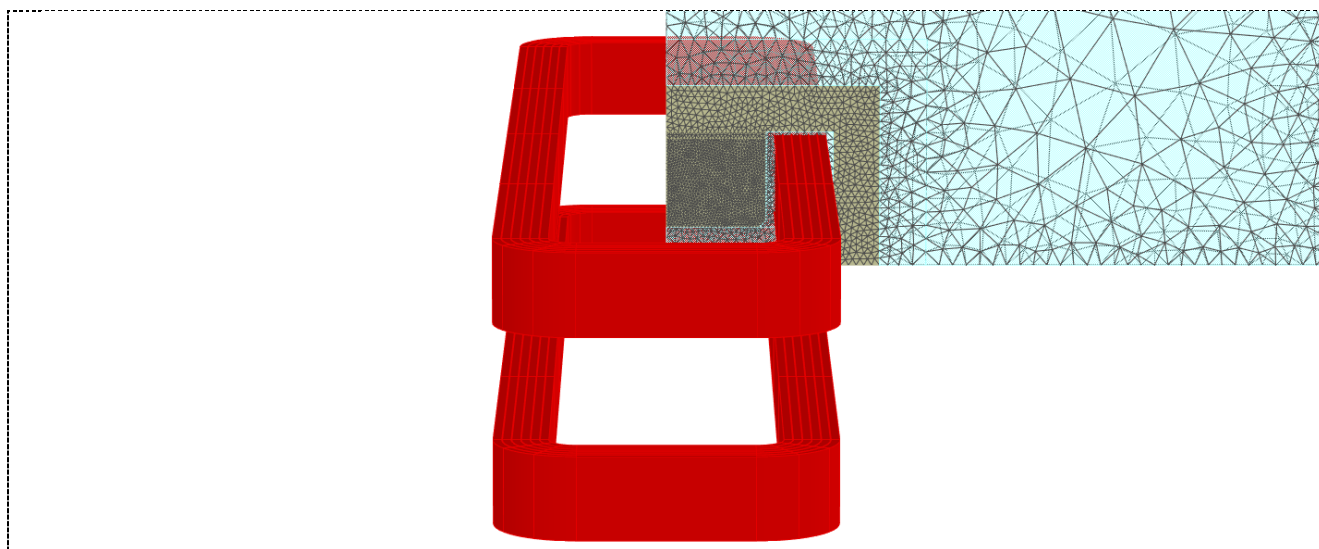


Figure 2: D1 2D5 model defined in Opera 3D

Since the dipole is symmetric with respect to all the planes (xy, yz and zx), the 2D5 simulation consists in a 3D simulation of only one quarter of a central slice of the yoke 1 mm thick (a single lamination sheet). In this way the 2D5 and 3D simulations are performed with the same finite elements algorithms and can be defined by the same list of commands (the Opera *.comi) for a better correspondence between the 2D5 and the 3D meshing and final results. The imposed boundary conditions of the magnetic flux lines are perpendicular to the y-axis, tangential to the x-axis and tangential to both the lamination sheet surfaces. The yoke material is defined with the BH curve mentioned in section 3.4 without packing factor.

Figure 2 shows the 2D5 simulation model defined in Opera 3D.

4.3 FIELD HOMOGENEITY OPTIMIZATION

In the 2D5 and 3D simulations, the harmonic content of the magnetic flux density is evaluated calculating the components of the values/integrals of the field on points/paths defined by the GFR on y/yz.

The goal was to minimize the pick-to-pick variation of the field values/integral along the points/paths of the GFR on y/yz.

The 2D5 and 3D optimizations were assumed completed when the pick-to-pick variation was smaller than what specified.

4.4 2D5 FIELD HOMOGENEITY OPTIMIZATION

Since the pole profile was preferred without any kind of shimming, the required field homogeneity can be obtained through the pole width only. The pole width effect has been studied via 2D5 simulations. Figure 3 shows the variation of the magnetic flux ΔB_x along the Y axis for several values of the pole width w .

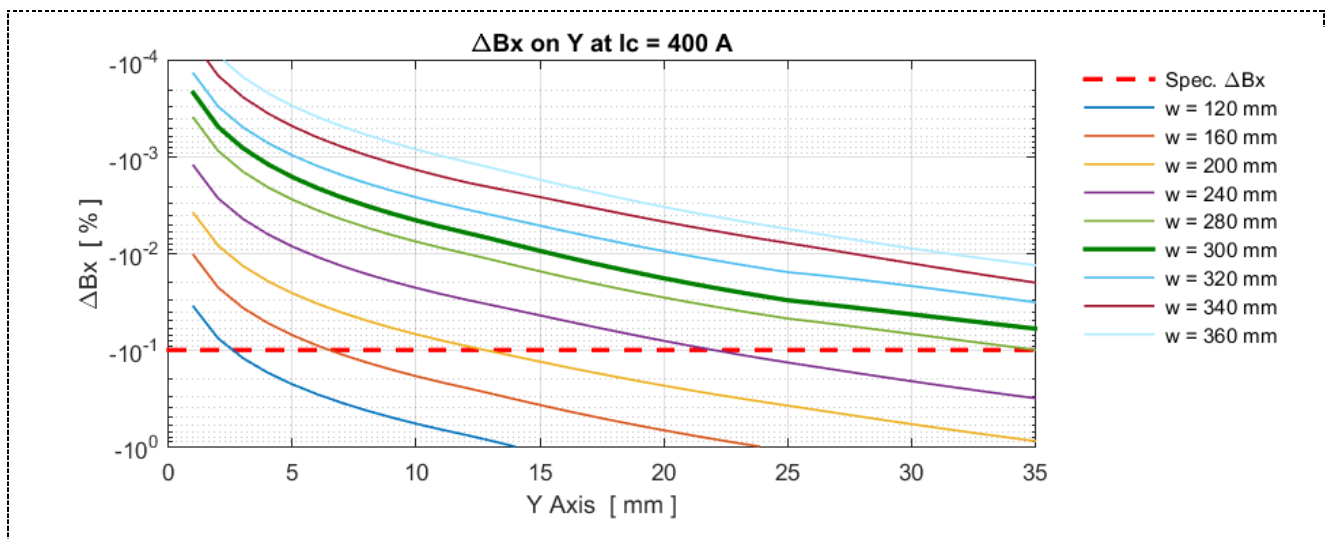


Figure 3: D1 pole width study

In order to obtain the required field homogeneity, it is clear (see Figure 3) that the pole width should be greater than 300 mm.

Another run of 2D5 simulations studied the effect of the frame with on the iron saturation.

Figure 4 shows the B field distribution on yoke for several values of the frame width, while Figure 5 shows the B_x field distribution (and performance) along the Y axis.

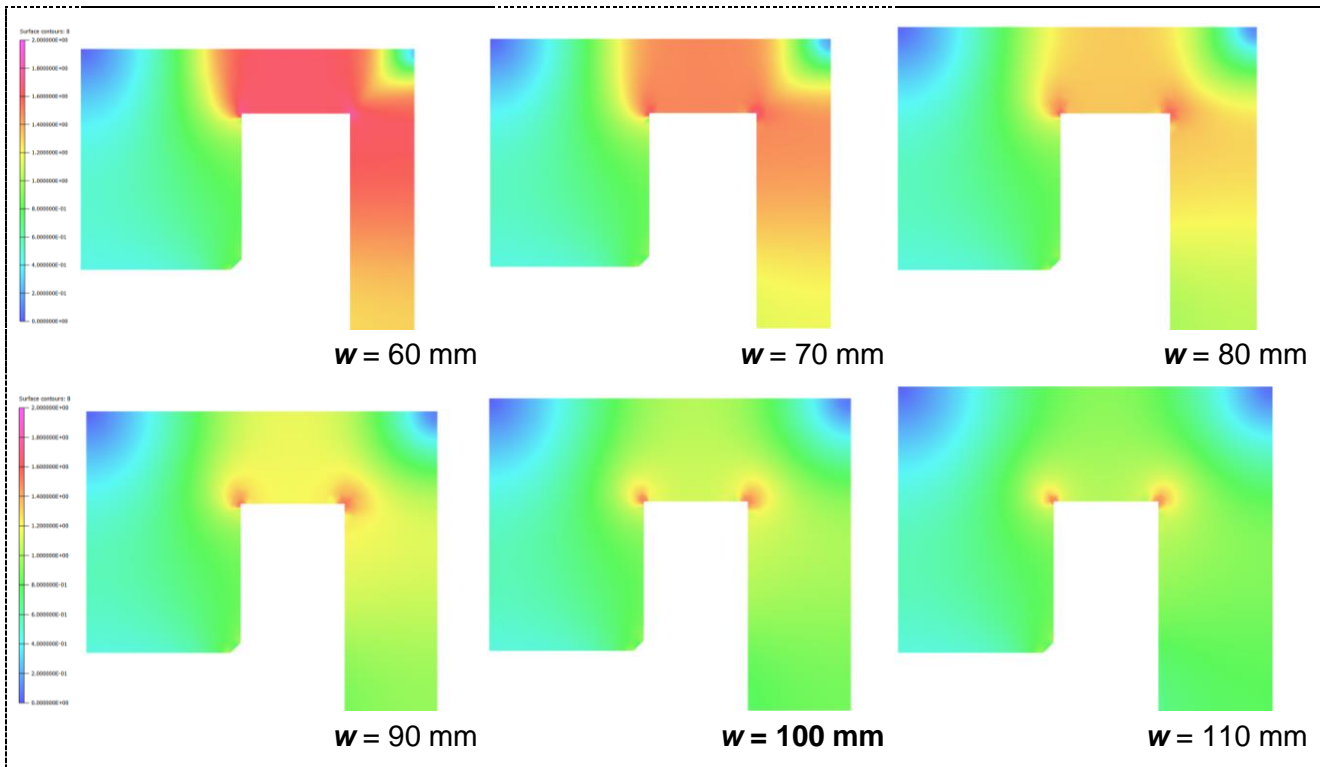


Figure 4: D1 frame width w study: B_{mod} field distribution on cross section. Colored bar from 0 to 2 Tesla

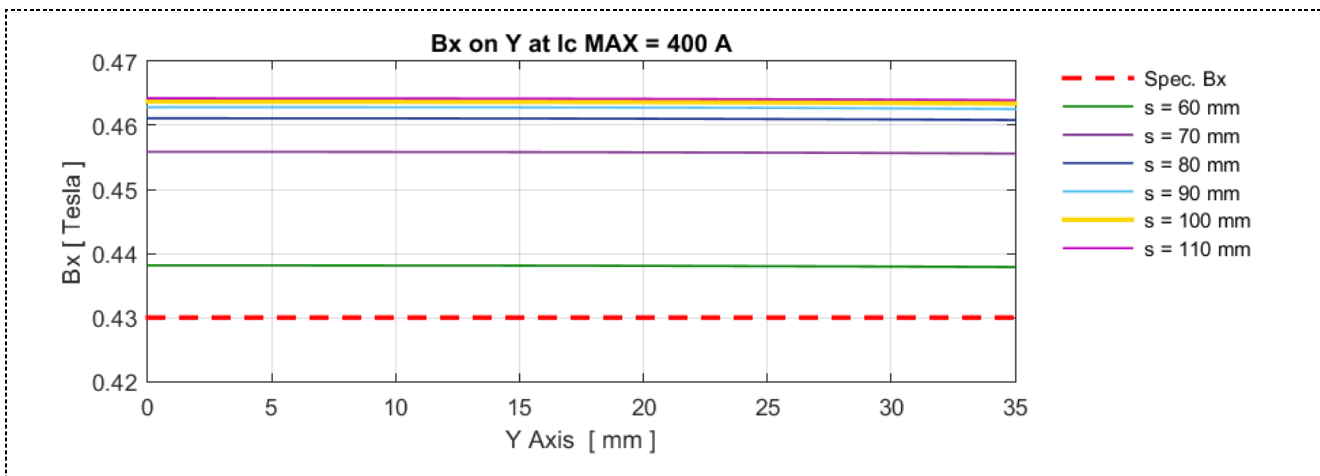


Figure 5: D1 frame width w study; B_x distribution along Y

From Figures 4 and 5 it is possible to observe that the smaller frame size reduces the magnet performance due to the iron saturation. It should be noted that the saturation on the frame has no effect on the field homogeneity.

In order to have more margin in terms of performance and yoke saturation (there could be some issues due to the closing system), the frame size should be equal to 100 mm.

4.5 3D SIMULATIONS

The 3D simulations have been used for pre-design and 3D harmonic optimization.

In the pre-design, the tridimensional calculations help the evaluation of the magnetic length, the ampere-turns performances and magnet inductance.

Since the dipole has a big aperture, the harmonic effect of the fringe field is not negligible and the final magnetic models need a 3D harmonic optimization.

The Opera 3D models use some of the symmetries adopted in the 2D5 simulations (only the plane YZ), plus the longitudinal symmetry on the plane XY. In this way the simulated model is one-fourth ($1/4^{\text{th}}$) of the whole dipole. The yoke material is defined via the BH curve mentioned in section 3.4 with a packing factor of 97%. The current density is defined including the intra-coils insulation thickness.

Since the 3D models need heavier calculations than the 2D5 models, different meshing sizes are evaluated in order to study more thoroughly the integrated field distribution.

Figure 6 shows the Opera 3D models of D1 yoke, coils and the GFR air box, that is curved in parallel to the nominal path. The other air regions are hidden.

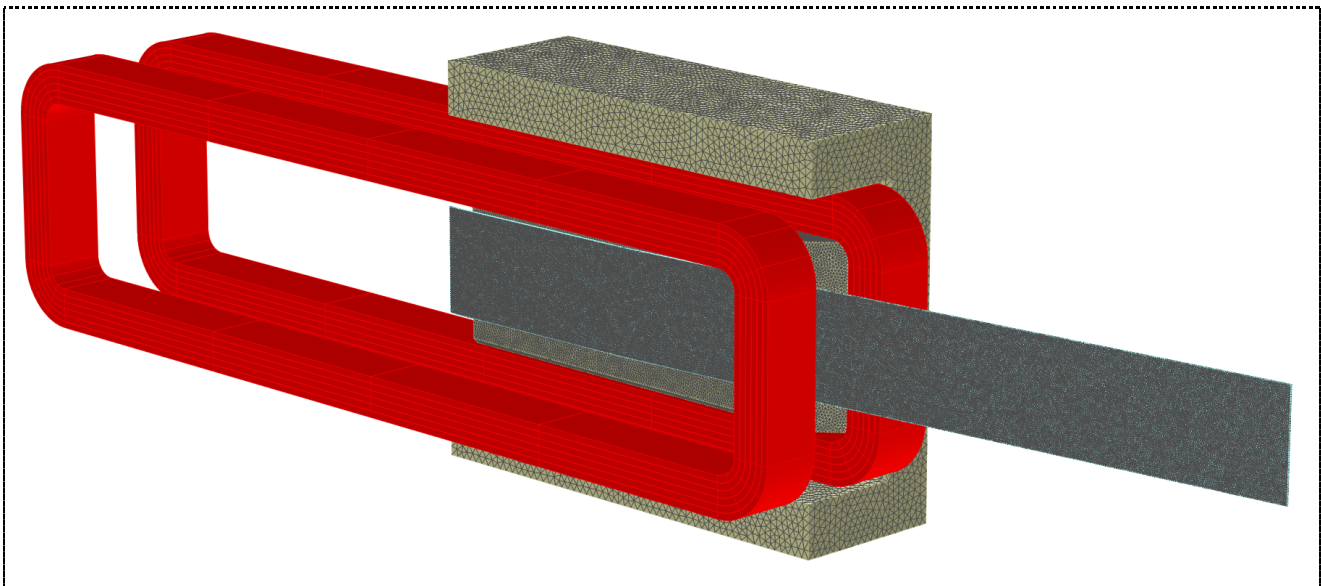


Figure 6: D1 3D model defined in Opera 3D

To note that the 3D pole terminations are worked with chamfers whose angle and size are calculated to interpolate the corresponding Rogowski surface.

4.6 3D FIELD HOMOGENEITY OPTIMIZATION

Having optimized the pole width by the 2D5 method, the 3D stage of the design process will check the effect of the fringe field on the integrated field homogeneity.

Figure 7 shows the integrated B_x field distribution along Y axis at the max current of 400 A.

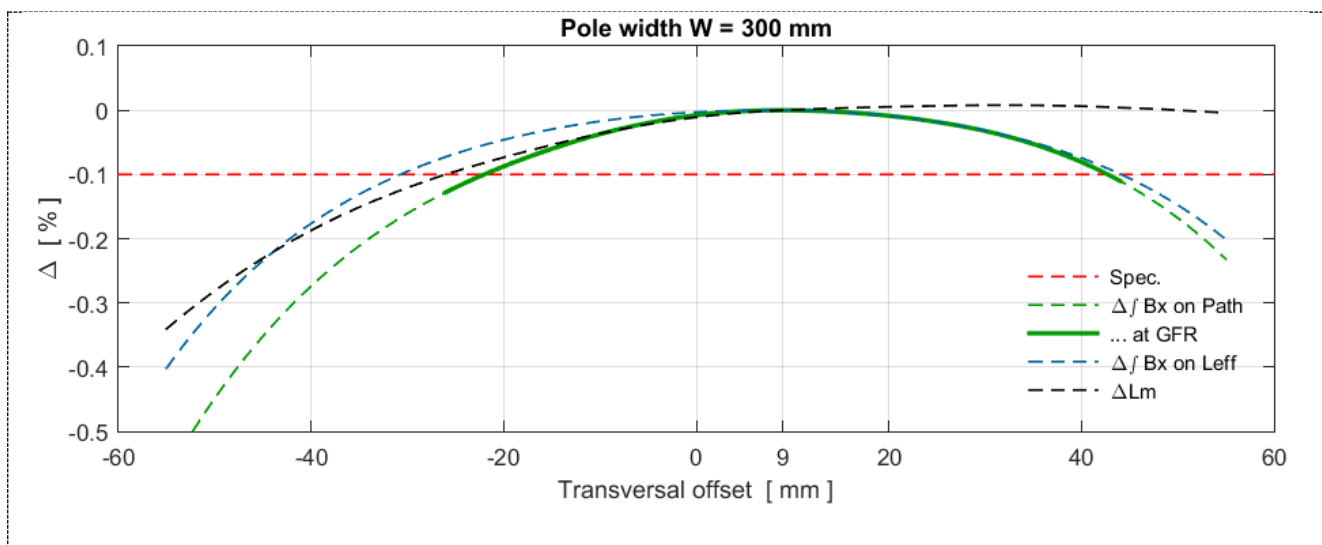


Figure 7: D1 B_x and L_{mag} distributions; Pole width of 300 mm

It should be noted that, due to the fringe field, the 2D5 field distribution is degraded with a new quadrupole component (B_2) and a bigger sextupole component (B_3). Even with an offset of 9 mm, the specified limit of -0.1% is not satisfied.

To increase the field homogeneity (in the 3D model) there are only two possibilities: increase the pole width or modify the pole terminations by a nonlinear 3D shimming.

Figure 8 shows the 3D yoke model with the mentioned solutions, while Figure 9 collects the integral field distribution in the two best cases of widening and shimming.

Since the integrated field homogeneity is satisfied by a very small increasing of the pole width (340 Vs 300 mm), this solution is preferable because the shimming on the ends could require too high mechanical precision. In addition, by the nonlinear 3D shimming, the homogeneity of the integrated field is mathematically matched by adding the integrated field on the nominal curve and that on the fringe. Because these are conflicting, it is not sure that the tracking of the particles leads to such a result.

The final proposed 3D model will have a pole width of 340 mm, without shimming on the pole ends.

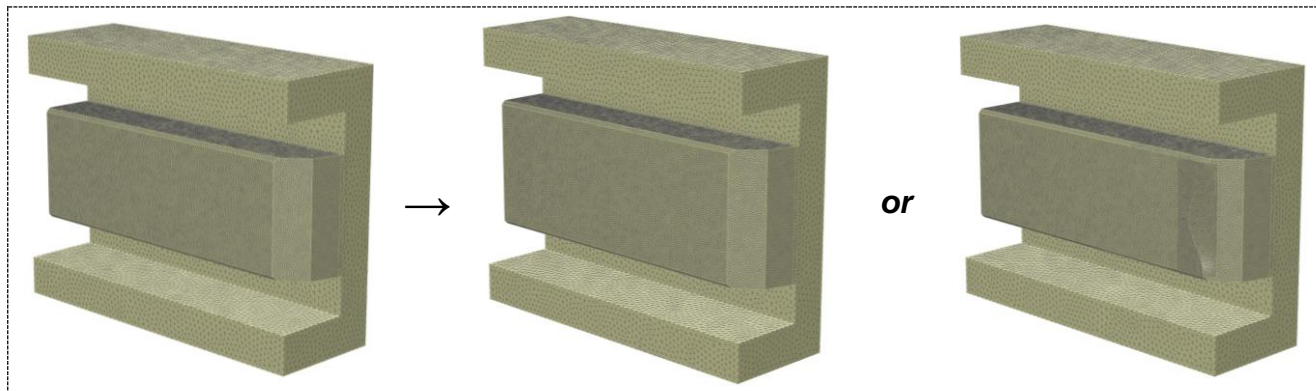


Figure 8: D1 yoke (1/4th) 3D models; original w , bigger w and original w with nonlinear shimming.

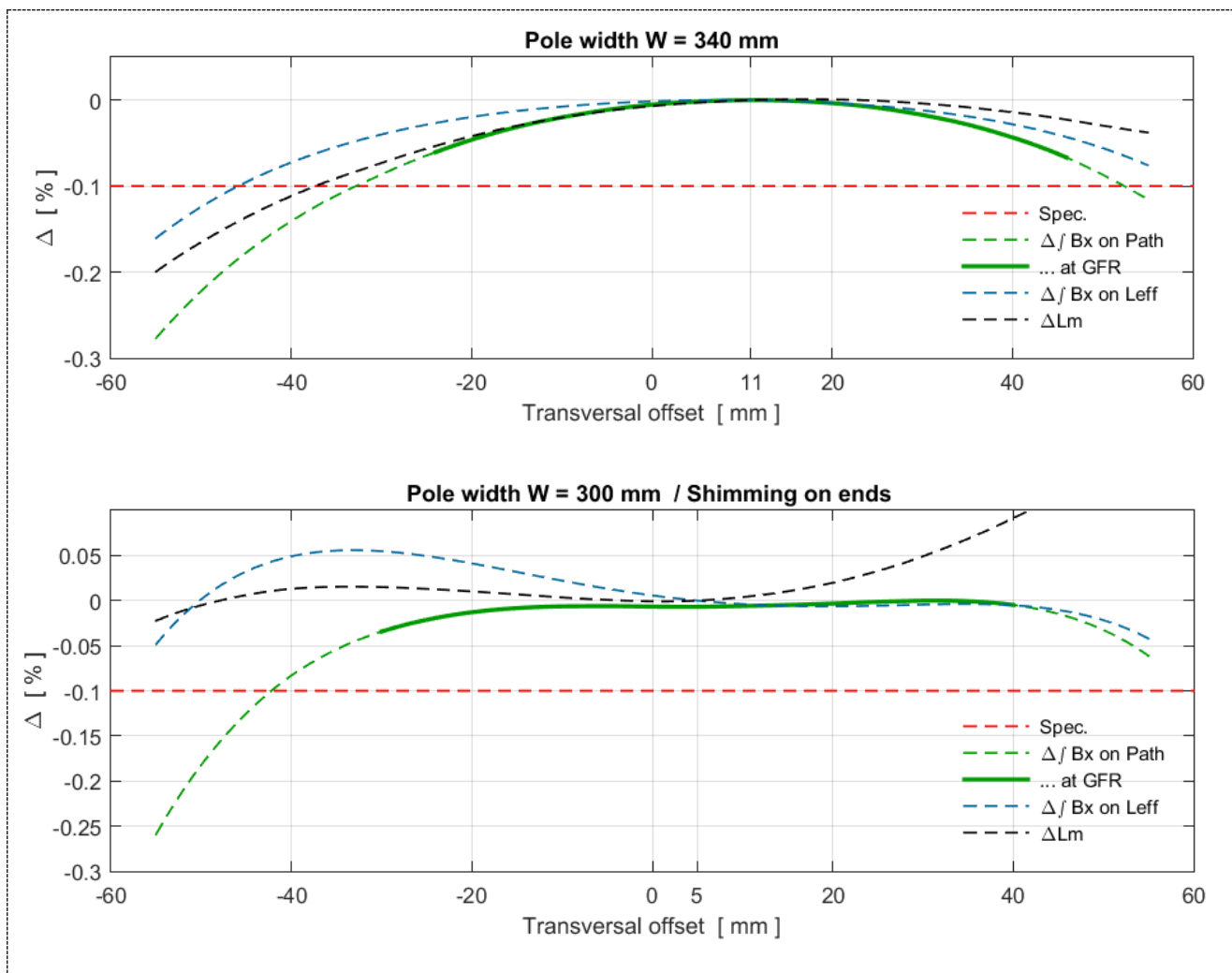


Figure 9: D1 $\int B_x$ and L_{mag} distribution results.

5 D1 SUMMARY

5.1 CONCEPTUAL 3D MODEL

The D1 conceptual model include the base yoke half and the proposed conductor windings of the main coil.

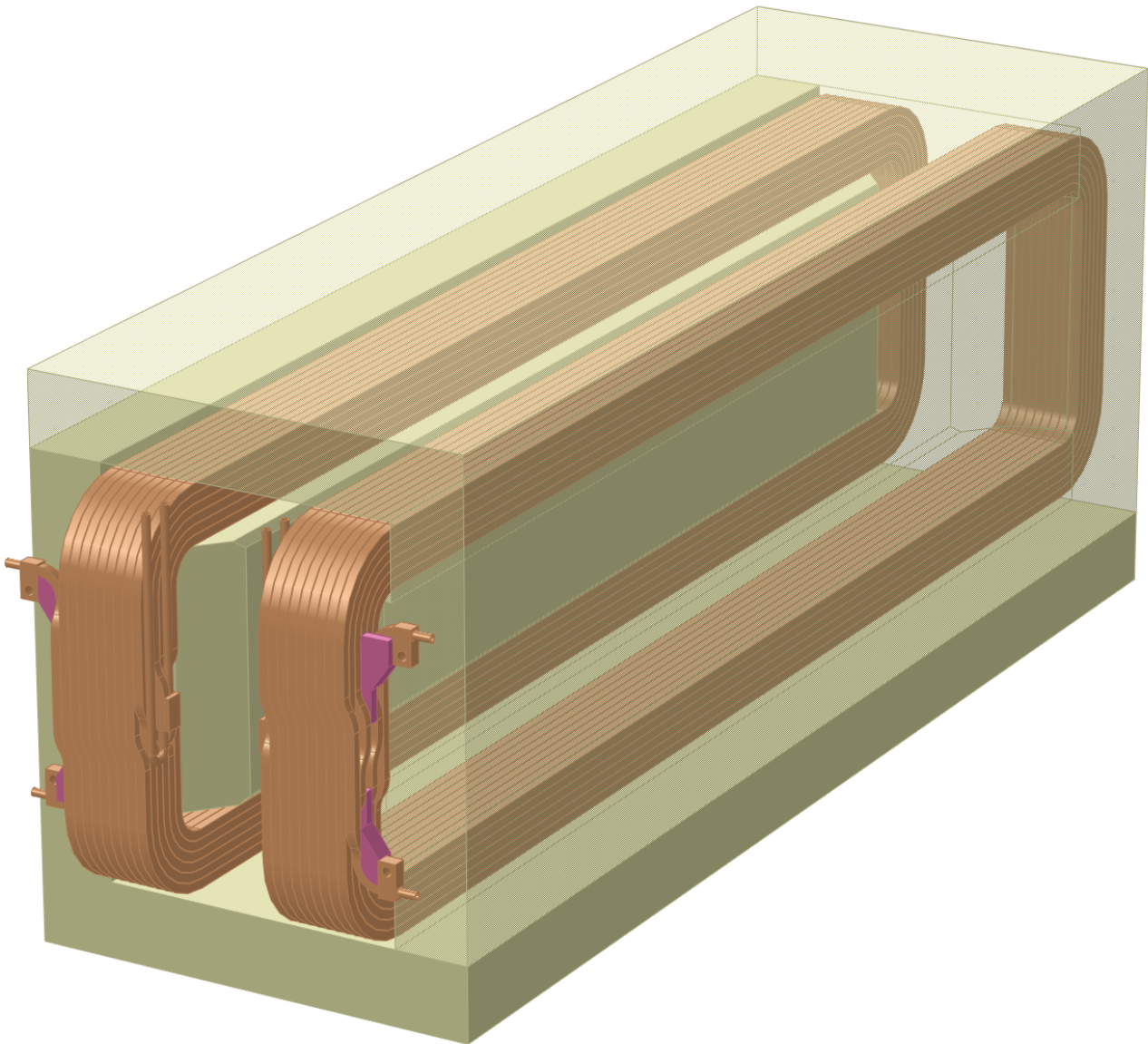


Figure 9: D1 conceptual model

The yoke could be added with some blocks for support and positioning of alignment. Since the yoke has a sufficient length, the electrical connection box and the cooling circuit manifolds (inlet and outlet) could be positioned on the same side.

5.2 Q5 MAGNETIC PERFORMANCES

In order to obtain consistent results, the D1 magnetic performances are calculated by Opera 3D for several excitation current values on the same model and exactly the same post processing. The meshing used for this simulation series is higher than the one used for the yoke parameters optimization and the relative pick-to-pick variations are accordingly slightly different. Table 7 lists the D1 magnetic performances.

Table 7: D1 magnetic performances; offset $y_0 = +15$ mm; $\int B_3$ and $\int B_2$ at $y = y_0 - R_{GFR} = -20$ mm.

	Curr [A]	B_0 [T]	$\int B$ [Tm]	L_{mag} [mm]	η [%]	$\int B_3 / \int B_1$	$\int B_2 / \int B_1$
	400	0.4644	0.8369	1801.98	-0.74	-7.4102e-4	3.2325e-5
nominal range	371	0.4307	0.7762	1801.98	-0.73	-7.4102e-4	3.2325e-5
	345	0.4006	0.7218	1801.98	-0.72	-7.4102e-4	3.2325e-5
	310	0.3599	0.6486	1801.98	-0.71	-7.4102e-4	3.2325e-5
	200	0.2322	0.4185	1801.98	-0.68	-7.4102e-4	3.2325e-5
	120	0.1394	0.2511	1801.98	-0.62	-7.4102e-4	3.2325e-5
	50	0.0581	0.1046	1801.98	-0.40	-7.4102e-4	3.2325e-5

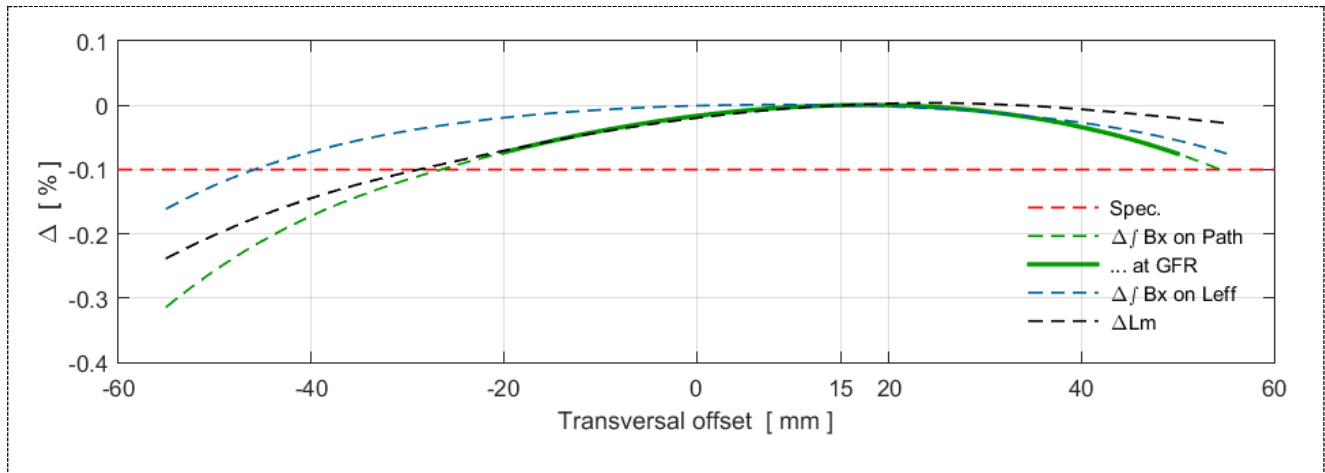


Figure 10: D1 proposed model; Field integral and L_{mag} distributions; offset $y_0 = +15$ mm

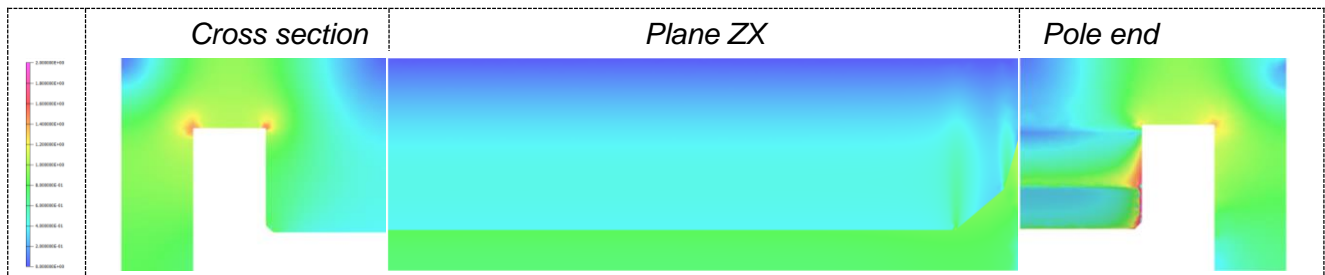


Figure 11: B_{mod} distribution on $1/8^{th}$ of the yoke, at 345 A (nominal max); colored bar from 0 to 2 Tesla

6 ANNEX

6.1 MATERIAL USED FOR MAGNETIC SIMULATIONS

The material used for the magnetic simulation is based on the Opera “tenten” data.

Table 8 lists the relative $B(H)$ data.

Table 8: $B(H)$ data of the steel type used for magnetic field simulation

B [Gauss]	H [Oersted]
0	0
5757	2.09
6800	2.5
7918	3.02
8949	3.63
9921	4.365
10821	5.248
11640	6.31
12373	7.586
13021	9.12
13586	10.96
14074	13.18
14494	15.85
15171	22.91
15451	27.54
15955	39.8
16455	57.54
17019	83.18
17679	120.23
18045	144.5
18432	173.8
18831	208.9
19236	251.2
19636	301.99
20022	363.08
20384	436.5
20713	524.8
21003	630.95
21251	758.7
21461	912
21646	1096.5
21869	1318.3
22137	1584.9
22458	1905

6.2 DIPOLE MODEL

The quadrupole 3D model could be exported in the step file format. The following page reports the base drawing of the model.

